Supporting Information

Wang et al. 10.1073/pnas.1317911111

Materials and Methods

Maintenance of Fly Stocks. All flies except those used in optogenetics experiments were reared on standard cornmeal–agar–molasses medium in small vials (Thermo Fisher Scientific) at ~25 °C, with relative humidity of ~50% and a 12 h/12 h light/dark cycle. Fly stocks used in this study and their origins are as follows: Gal4/UAS lines are *GH146-Gal4* (1); *Mz699-Gal4* and *Mz19-Gal4* (2, 3); *Np839-Gal4*, *Np1580-Gal4*, *Np2331-Gal4*, and *Np7365-Gal4* (4); *UAS-mCD8-GFP* (5); and *UAS-G-CaMP3* (6). QF/QUAS lines are *GH146-QF* and *QUAS-tdTomato* (7). LexA/LexAop lines are *Orco-LexA::VP16* and *GH146-LexA::GAD* (5); *LexAop-G-CaMP1.6* (8); *LexAop-G-CaMP3* (9); and *LexAop(optimized)-G-CaMP3* (10). FRT/FLP lines are *Tub-FRT-Gal80-FRT*, *hs-FLP,MKRS/TM6B*, and *hs-FLP,Sco/CyO* (11). The $shakB^2$ mutant was characterized previously (12) and was a gift from R. J. Wyman (Yale University, New Haven, CT). *UAS-ChIEF-tdTomato*, *QUAS-ChIEF-tdTomato*, *UAS-R-GECO1*, and *QUAS-R-GECO1* transgenic flies were generated in the Zuoren Wang laboratory. Some flies were cultured at 30 °C to shorten the time required to generate specific genotypes.

Generation of Transgenic Flies. To create the *pUAST-R-GECO1* and *pQUAST-R-GECO1* constucts, the coding sequence of *R-GECO1* was amplified from the plasmid *CMV-R-GECO1* obtained from Addgene and subcloned into plamids *pUAST* and *pQUAST*, respectively. Transgenic flies were generated by injecting the constructs into w^{1118} embryos with a helper plasmid, crossing the injected flies with w^{1118} flies, and selecting the positive offspring according to eye colors. Transgenic lines with high expression levels and minimal leaky expression were chosen in this study. To increase the expression level of R-GECO1, alleles with two copies of *UAS-R-GECO1* inserted at different loci on the same chromosome were used.

Mosaic Analysis of *Mz699-Gal4*. To label a subset of neurons in the *Mz699-Gal4* line, females of the *Tub-FRT-Gal80-FRT; UAS-mCD8-GFP; Mz699-Gal4* genotype were crossed to males of *Sco, hs-FLP/CyO; GH146-QF,QUAS-tdTomato*, and their offspring were heat shocked in a 37 °C incubator for 0.5 h at different developmental stages. Offspring not carrying balancer *CyO* were selected and examined. To label single neurons in the *Mz699-Gal4* line, FLP-out was performed by crossing *Tub-FRT-Gal80-FRT; UAS-mCD8-GFP; Mz699-Gal4* females with *UAS-mCD8-GFP; MKRS,hs-FLP/TM6B* males, or by crossing *Tub-FRT-Gal80-FRT; UAS-G-CaMP3; Mz699-Gal4,UAS-G-CaMP3* females with *UAS-G-CaMP3; MKRS, hs-FLP/TM6B* males. Their offspring were heat shocked in a 37 °C incubator for 1–2 h at different developmental stages. Offspring carrying *MKRS* but not balancer *TM6B* were selected and examined.

Electrophysiology. Our recording equipment is set up on an upright FN1 microscope (Nikon). Recordings were performed at 22–25 °C with a Multiclamp 700B amplifier (Molecular Devices) using low-resistance pipettes (12–15 MΩ for whole-cell recording on *Mz699-Gal4*–labeled mediolateral tract projection neurons, or mlPNs and lateral horn neurons, 9–12 MΩ for whole-cell recording on other antennal lobe neurons, 6–10 MΩ for loose-patch recording on medial tract projection neurons, mPNs). The data were low-pass filtered at 2 kHz and acquired at 10 kHz with a Digidata 1440A digitizer (Molecular Devices). All reagents were purchased from Sigma-Aldrich unless otherwise indicated.

To perform ex vivo recordings, flies ages 3–5 d were immobilized by cooling on ice for 15–30 s, and their brains were dissected out in extracellular solution, which contained (in millimoles): 103 NaCl, 3 KCl, 5 *N*-Tris(hydroxymethyl) methyl-2-aminoethanesulfonic acid, 10 trehalose, 10 glucose, 2 sucrose, 26 $NaHCO_3$, 1 NaH_2PO_4, 1.5 $CaCl_2$, and 4 $MgCl_2$ [pH near 7.3 when bubbled with 95% (vol/vol) O_2/5% (vol/vol) CO_2, ~295 mOsm] (13). The fat and trachea were removed, and then a small opening was made on the perineural sheath around the antennal lobe (AL) or the lateral horn (LH) with fine forceps (Fine Science Tools) to ensure the least damage to neurons in these regions. With nylon fibers tied on a U-shape platinum, the brains were positioned with their ALs upward, allowing access for the electrodes. Brains with any damage in the neuropil or with many neurons lost were not used. For whole-cell patch-clamp recordings, the intracellular solution contained (in millimoles) 140 K-gluconate, 10 Hepes, 1 KCl, 4 MgATP, 0.5 Na_3GTP, 1 EGTA, and 0.5–1% biocytin hydrazide or neurobiotin (Vector Laboratories) (pH near 7.3, ~285 mOsm). In most recorded neurons, a small constant hyperpolarizing current (0–20 pA) was injected to keep the membrane potential between −65 and −60 mV. For loose-patch recordings, the pipettes were filled with extracellular solution, and seals of 50–100 MΩ were formed by gentle suction.

In the experiment where stimulation of the antennal nerve was required, the brains were dissected out after acute ablation of the second and third segments of the antennae, a manipulation that usually preserves long bundles of the antennal nerve. To stimulate the antennal nerve, a suction pipette with a diameter of 5–8 μm at the opening and filled with extracellular solution was used to hold the end of the nerve bundle. Pulsed electrical stimulations were provided by linking the suction pipette with an ISO-FLEX isolator (A.M.P.I.) controlled by Digidata 1440A.

Calcium Imaging. Calcium imaging was performed at 20–22 °C under a Nikon-FN1 confocal microscope with a Nikon NIR Apo 40× water immersion objective (N.A. = 0.8) or a Nikon Apo LWD 25× water immersion objective (N.A. = 1.1). Adult females ages 7–28 d were immobilized by cooling on ice and then inserted into a rectangular hole (1.8 mm × 1.0 mm) at the bottom of a custom-made recording chamber. The fly's body was adjusted to be horizontal and the antennae and proboscis were beneath the chamber. A small amount of Loctite 352 light cure adhesive (Henkel) was used to fix the fly in place and cured with 15 s of UV illumination. After the chamber was filled with extracellular solution, a window was opened in the dorsal head cuticle with fine forceps to expose the dorsal part of the brain. Some fat and trachea at the dorsal part of the brain were also gently removed. In some preparations, the esophagus was ablated to minimize the movement of the brain. The flies were alive during the experiment (~2 h) with spontaneous leg movements.

In single-color calcium-imaging experiments, laser light of a single wavelength (473 nm or 561 nm) was used to illuminate brain regions of interest. In dual-color imaging experiments, lasers of 473 nm and 561 nm were applied simultaneously. Images were captured in time series at 2 or 4 Hz with a resolution of 256 × 128 pixels for ALs or a resolution of 128 × 128 pixels for LH. The thickness of the optic section was 8 μm at AL and 4 μm at the LH. To examine the activity of large parts of ALs and LHs, image series were taken at different depths with intervals of 10 μm or 4 μm, respectively. High-speed imaging with dual colors was facilitated by an acousto-optic tunable filter (AOTF) laser control. After odor stimulation, a high-resolution image stack (1-μm interval) of the ALs or LH was acquired at 1,024 × 512 pixels or 512 × 512 pixels, respectively.

To calculate the response amplitude, regions of interest (ROIs) were selected in the Fiji image-analysis program (13). Absolute fluorescence intensity changes (dF) and fluorescence changes relative to baseline fluorescence intensity (dF/F_0) in defined ROIs were calculated by programs written in MATLAB (MathWorks). For odor-evoked fluorescence responses containing both increase and decrease phases, the sum of fluorescence changes ($\Sigma dF/F_0$) during a defined period was calculated.

Odor Stimulation. Most odors were diluted at a ratio of 1:100–1:10,000 (vol/vol) in paraffin oil and contained in glass vials. To present the pheromone 11-cis-Vaccenyl acetate (cVA), a filter paper containing 10 μL synthetic cVA (Pherobank) was placed at the output path of a paraffin-oil–containing glass vial. The odor stimulation was given by a custom-built odor delivery system, which is composed of 38 three-way solenoid valves (Shinyeong Mechatronics) controlled by a PCI-6221 data acquisition board (National Instruments). Programs written in MATLAB were used to provide odor-stimulation orders. A constant airflow (~500 mL/min) was provided at the front of the fly throughout the recording, and a fraction of the air stream (20–50% adjusted with two flow meters) was redirected to one vial containing a specific odor for a desired period (1–2 s), with start-to-start intervals of 10–20 s. The odor stream and the main air stream rejoined at ~10 cm from the end of the delivery tube, which was positioned ~1 cm away from the head of the fly. A small fan was placed in front of the fly to quickly remove the odors.

Optogenetic Stimulation. Flies used in optogenetic activation experiments were cultured on standard food plus 100 nM *all-trans*-retinal. *All-trans*-retinal was prepared as a stock solution in ethanol (100 mM) and diluted 10^6-fold by mixing it with the melting food when the temperature was lower than 50 °C. Flies were reared under faint illumination with a 12/12 h light/dark cycle.

To selectively illuminate the samples, we used a 473-nm blue laser (Changchun New Industries Optoelectronics Technology) and a custom-built acousto-optic system (CBBMP) which can steer a focused laser spot (~1.4 μm in diameter under a Nikon, NIR Apo 40×/0.80w objective) to different locations in the field (e.g., hundreds of spots covering one antennal lobe) in an ultrafast manner (refresh rate = 5,000 Hz). An IR-1000E CCD camera (DAGE-MTI) and an image grabber were used to capture images of the samples. ROIs were selected with Image-Pro Plus (Media Cybernetics) and the position information was saved. Then a program written in Labview (National Instruments) was used to control the acousto-optic deflector (AOD) system to synthesize desired illumination patterns (e.g., ROIs, illumination length, and laser intensity). In addition to laser stimulation, blue or green light from an arc lamp was used to provide wide-field illumination.

Fluorescent Immunostaining. All of the immunostaining was performed following a similar protocol. In brief, brains were fixed in PBS with 4% paraformaldehyde at 25 °C for 15 min, and blocked for 1 h at 25 °C in PBS containing 0.3% Triton X-100 and 10% heat-inactivated normal goat serum. Then the brains were incubated with primary antibodies diluted in blocking buffer either at 25 °C for ~6 h or at 4 °C for 24–72 h. After washes in PBS containing 0.3% Triton X-100 for several hours at 25 °C, the brains were further incubated with secondary antibodies at 4 °C for 24 h. Then, the brains were washed in PBS at 25 °C for 30 min and mounted in Vectashield (Vector Laboratories).

The primary antibodies used were mouse nc82 antibody [1:50 (vol/vol); Developmental Studies Hybridoma Bank, or DSHB] to visualize brain structures, rabbit anti-GABA antibody (1:500; Sigma-Aldrich) to stain GABAergic neurons, mouse anti-ChAT antibody [1:50 (vol/vol); DSHB] to stain cholinergic neurons, rhodamine-conjugated avidin (1:500; Vector Laboratories), or Alexa Fluor 633-conjugated streptavidin (1:500; Invitrogen) to visualize the morphology of neurons filled with biocytin or neurobiotin, and rabbit anti-GFP antibody (1:500; Invitrogen) to enhance the signal of GFP.

The secondary antibodies used were goat anti-mouse Alexa Fluor 405 and Alexa Fluor 633 (1:200; Invitrogen); goat anti-rabbit Alexa Fluor 488, Alexa Fluor 546, and Alexa Fluor 633 (1:200; Invitrogen); rhodamine-conjugated avidin (1:500, Vector Laboratories); and Alexa Fluor 633-conjugated strepavidin (1:500; Invitrogen).

Confocal Microscopy and Image Processing. Confocal imaging was performed under a Nikon FN1 upright confocal microscope, with a Nikon S Fluor 40× oil immersion objective (N.A. = 1.3) or a Nikon NIR Apo 40× water immersion objective (N.A. = 0.8) and lasers with wavelengths of 405 nm, 473 nm, 561 nm, and 637 nm. The thickness of the optic section was 0.6 μm or 1.2 μm. High-resolution Z stacks (1,024 × 1,024 pixels or 2,046 × 2,046 pixels) with an interval of 1.2 μm or 2.5 μm were taken. Software including Fiji (14) and Photoshop (Adobe) was used to process captured images.

Behavioral Assays. All flies used in behavioral assays were backcrossed for four generations with the w^{1118} flies kept in our laboratory. To avoid overcrowding, parent flies were reared in each vial at a density of 7–10 pairs. After every 2–3 d of egg laying, parents were moved into new vials containing fresh food. Offspring were collected by gentle aspiration or under light CO_2 anesthesia within 6 h after eclosion. Males were reared individually, whereas females were kept in groups of 8–10 animals. Flies were examined when 5–7 d old.

Pairing assay. Pairing assays were performed under white light illumination. Two individually reared males were sequentially introduced into a courtship chamber made of acrylic (diameter, 1 cm; height, 0.3 cm) by gentle aspiration, and the behavior of the pair was recorded by CCD cameras with a refresh rate of 25 Hz. Pairs of different genotypes were recorded simultaneously under different CCD cameras, and videos were manually analyzed offline. For each pair, a 10-min time window, which began at the first detection of unilateral wing extension, was analyzed, and the time when courtship or aggressive behaviors occurred was logged. The courtship index (CI) is the percentage of time during which a fly exhibits courtship behaviors, including chasing, unilateral wing extension (UWE), licking, and attempted copulation. The UWE index is the percentage of time during which unilateral wing extension was observed.

Courtship preference assay. Courtship preference assay was performed under dim red light. One individually reared tester male was introduced into a courtship chamber by gentle aspiration and left alone for 5 min. Two decapitated target flies, a Canton-S male and a Canton-S female, were then presented to the tester. Videos were taken and analyzed as in the pairing assays. The courtship preference index (PI) was calculated as $(CI^{female} - CI^{male})/(CI^{female} + CI^{male}) \times 100\%$.

Locomotion. A single male was introduced into a small chamber by gentle aspiration and its movement was video recorded. The movement was traced and the walking speed was calculated by using the software Ethovision (Noldus).

Statistical Analysis. MATLAB and Microsoft Excel (Microsoft) were used for statistical analysis. After testing the normality of the data distribution with the Kolmogorov–Smirnov test, a Student's *t* test or Wilcoxon rank sum test was used to compare the differences between groups, with *P* values of less than 0.05 considered as statistically significant.

1. Stocker RF, Heimbeck G, Gendre N, de Belle JS (1997) Neuroblast ablation in Drosophila P[GAL4] lines reveals origins of olfactory interneurons. *J Neurobiol* 32(5): 443–456.
2. Ito K, Sass H, Urban J, Hofbauer A, Schneuwly S (1997) GAL4-responsive UAS-tau as a tool for studying the anatomy and development of the Drosophila central nervous system. *Cell Tissue Res* 290(1):1–10.
3. Ito K, et al. (1998) The organization of extrinsic neurons and their implications in the functional roles of the mushroom bodies in Drosophila melanogaster Meigen. *Learn Mem* 5(1-2):52–77.
4. Tanaka NK, Endo K, Ito K (2012) Organization of antennal lobe-associated neurons in adult Drosophila melanogaster brain. *J Comp Neurol* 520(18):4067–4130.
5. Lai SL, Awasaki T, Ito K, Lee T (2008) Clonal analysis of Drosophila antennal lobe neurons: Diverse neuronal architectures in the lateral neuroblast lineage. *Development* 135(17):2883–2893.
6. Tian L, et al. (2009) Imaging neural activity in worms, flies and mice with improved GCaMP calcium indicators. *Nat Methods* 6(12):875–881.
7. Potter CJ, Tasic B, Russler EV, Liang L, Luo L (2010) The Q system: A repressible binary system for transgene expression, lineage tracing, and mosaic analysis. *Cell* 141(3): 536–548.
8. Root CM, et al. (2008) A presynaptic gain control mechanism fine-tunes olfactory behavior. *Neuron* 59(2):311–321.
9. Yao Z, Macara AM, Lelito KR, Minosyan TY, Shafer OT (2012) Analysis of functional neuronal connectivity in the Drosophila brain. *J Neurophysiol* 108(2):684–696.
10. Pfeiffer BD, et al. (2010) Refinement of tools for targeted gene expression in Drosophila. *Genetics* 186(2):735–755.
11. Gordon MD, Scott K (2009) Motor control in a Drosophila taste circuit. *Neuron* 61(3): 373–384.
12. Curtin KD, Zhang Z, Wyman RJ (2002) Gap junction proteins are not interchangeable in development of neural function in the Drosophila visual system. *J Cell Sci* 115(Pt 17):3379–3388.
13. Wilson RI, Laurent G (2005) Role of GABAergic inhibition in shaping odor-evoked spatiotemporal patterns in the Drosophila antennal lobe. *J Neurosci* 25(40): 9069–9079.
14. Schindelin J, et al. (2012) Fiji: An open-source platform for biological-image analysis. *Nat Methods* 9(7):676–682.

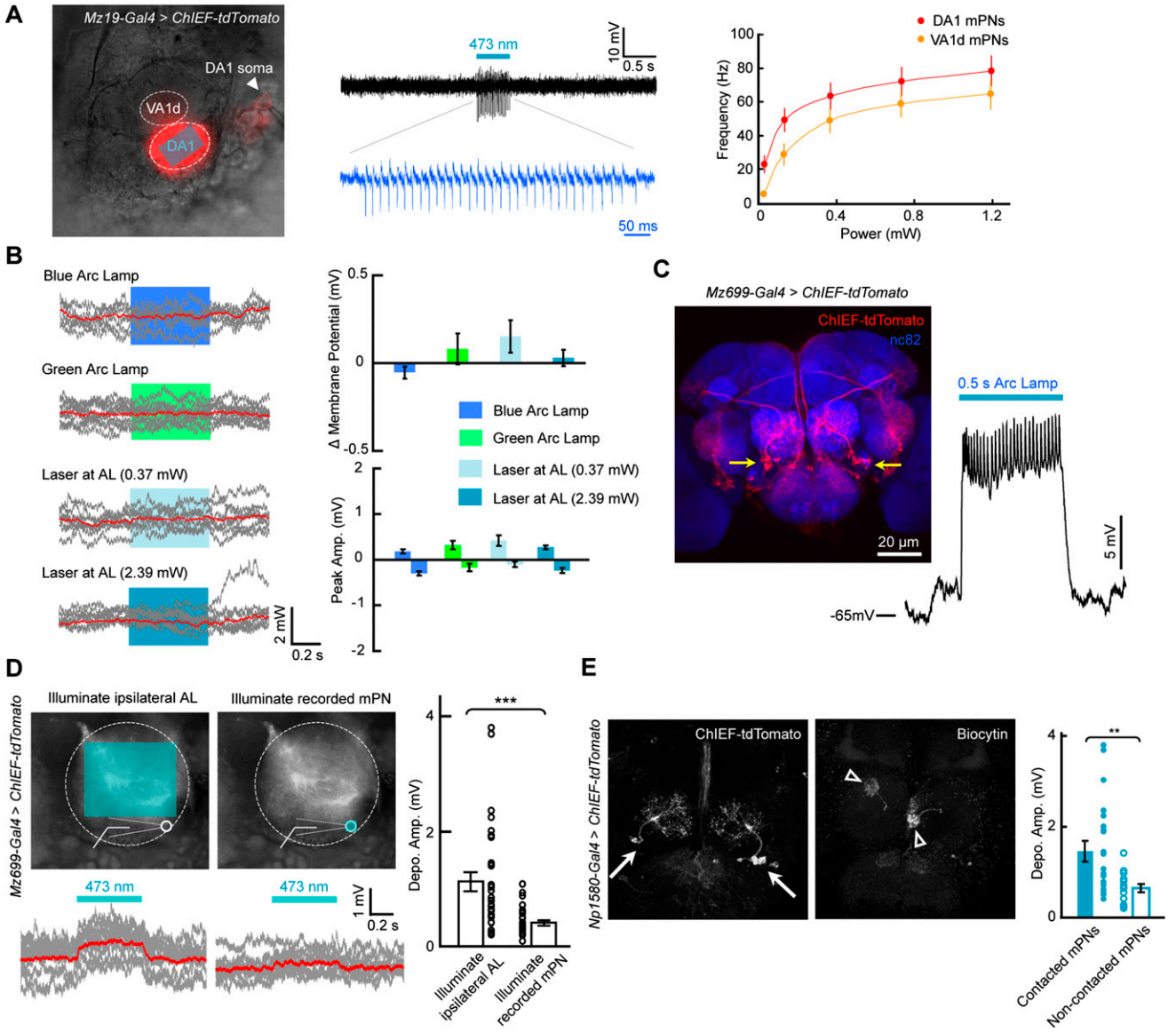

Fig. S1. Optogenetic activation of medial antennocerebral tract projection neurons (mPNs) and mediolateral antennocerebral tract projection neurons (mlPNs). (*A*, *Left*) Fluorescence image of an ex vivo AL in which the ChIEF-tdTomato fusion protein, which is an improved version of channelrhodopsin with a large plateau conductance and a fast closing rate, (red) is expressed in ∼13 mPNs innervating the three glomeruli labeled in *Mz19-Gal4* (dashed circles indicate DA1 and VA1d glomeruli, with DC3 glomerulus beneath VA1d glomerulus). A loose patch was performed on a DA1 mPN (arrowhead). (*Center*) Sample traces obtained from the loose patch on the DA1 mPN. Laser illumination of the DA1 glomerulus evoked spike trains. (*Right*) The frequency of laser-evoked spiking in DA1 and VA1d mPNs is plotted against the laser intensity, showing efficient optogenetic stimulation of ChIEF-positive mPNs (solid circles, mean; error bars, ± SEM, $n = 6$ each). (*B*) Sample traces (*Left*) and bar plots (*Right*) showing that light illumination (wide-field illumination with an arc lamp or restrictive illumination by laser) on the AL in brains without ChIEF expression evoked no obvious response in the recorded mPNs (mean ± SEM, $n = 15$). Both the positive and negative peak currents evoked by light stimulations were plotted. (*C*, *Left*) Fluorescence image showing a brain in which ChIEF-tdTomato (red) was expressed in *Mz699-Gal4*–labeled neurons, including a large fraction of mlPNs (arrows). The brain was counterstained with the nc82 antibody (blue). (*Right*) sample trace of whole-cell recordings performed on ChIEF-positive mlPNs. Blue light illumination of the ipsilateral AL (blue bars, 0.5 s) evoked depolarization and spiking in these mlPNs. (*D*) Fluorescence images and sample traces (*Left*) show that restrictive laser illumination (blue shaded area) of the AL (dashed circle) but not of the recorded mPN soma (open circle) caused marked depolarization, with plots (*Right*) summarizing peak depolarization amplitude caused by the indicated illumination patterns ($n = 31$ per group). (*E*, *Left*) Two fluorescence images showing an AL with ChIEF-tdTomato expressed in several mlPN2s (arrows) labeled by *Np1580-Gal4*, as well as biocytin loaded into two mPNs by whole-cell recordings (open arrowheads indicate the glomeruli innervated by recorded mPNs). (*Right*) Plots showing that optogenetic activation of mlPN2s labeled in *Np1580-Gal4* brains resulted in depolarizations in the indicated mPNs ($n = 20$ for contacted mPNs, $n = 16$ for noncontacted mPNs). Data in plots are shown as mean ± SEM; $^{**}P < 0.01$; $^{***}P < 0.001$.

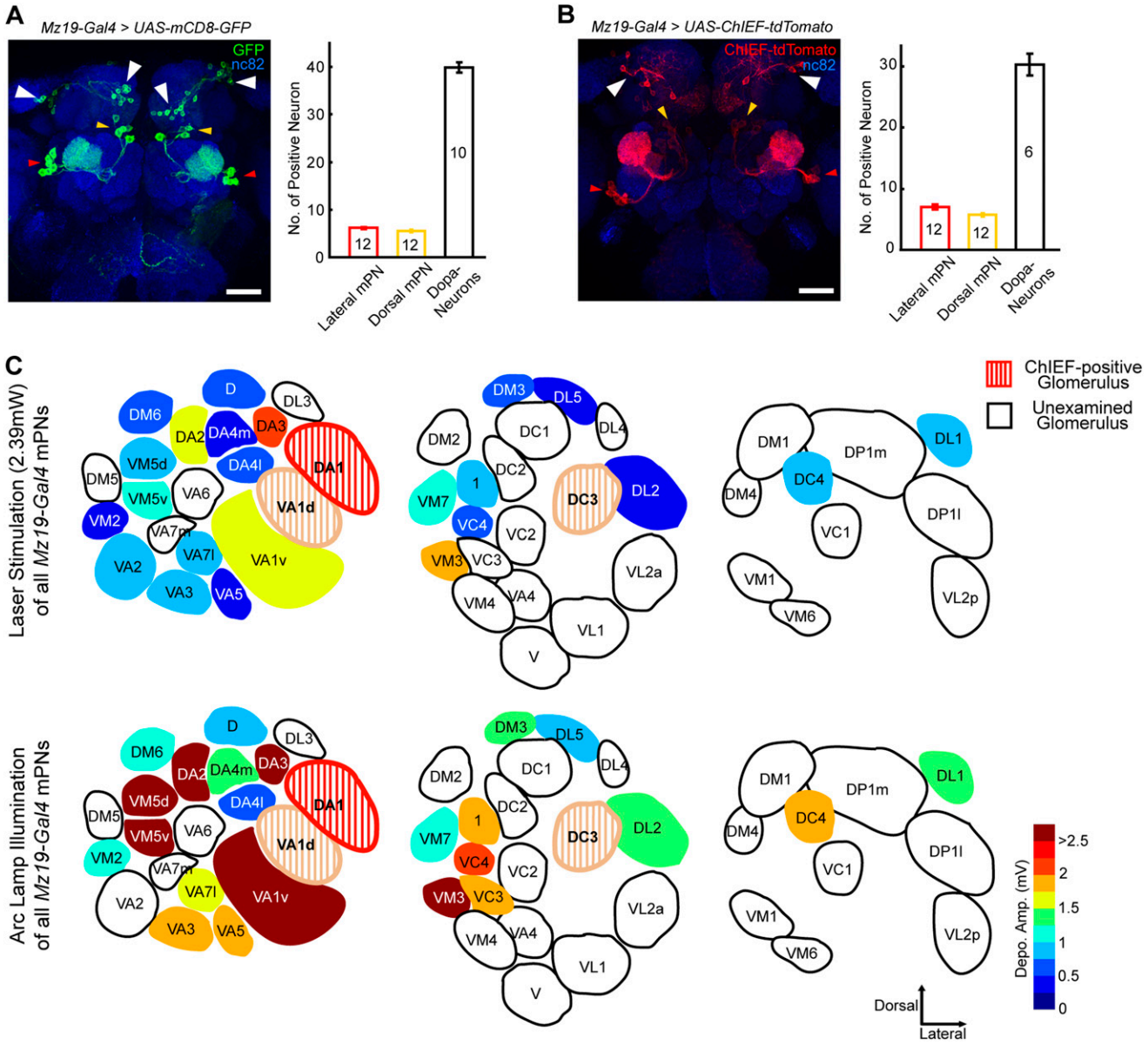

Fig. S2. Interglomerular crosstalk among heterotypic mPNs. (*A* and *B*) Sample images showing brains in which GFP (*Left*) or ChIEF-tdTomato (*Right*) was expressed under the control of *Mz19-Gal4*, with arrowheads indicating three clusters of neurons (red, lateral mPNs; yellow, dorsomedial mPNs; white, dopaminergic neurons). (Scale bars, 20 μm.) Bar plots (mean ± SEM) summarizing the average cell numbers, with sample numbers within the bars. (*C*) The mPNs labeled in *Mz19-Gal4* line (mPNs innervating the DA1, VA1d, and DC3 glomeruli) were activated optically as indicated, and responses in ChIEF-negative heterotypic mPNs were measured. Depolarization amplitudes recorded from ChIEF-negative heterotypic mPNs are coded in the colors indicated in the scale (*Lower Right*). The glomeruli of the *Left* AL are schematically illustrated in three anterior-to-posterior sections (reprinted from ref. 1, with permission from Elsevier, www.sciencedirect.com/science/journal/09609822). For each examined glomerulus, one to five PNs were recorded and the mean is indicated. Amplitudes of the mPNs in white glomeruli were not examined.

1. Couto A, Alenius M, Dickson BJ (2005) Molecular, anatomical, and functional organization of the Drosophila olfactory system. *Curr Biol* 15(17):1535–1547.

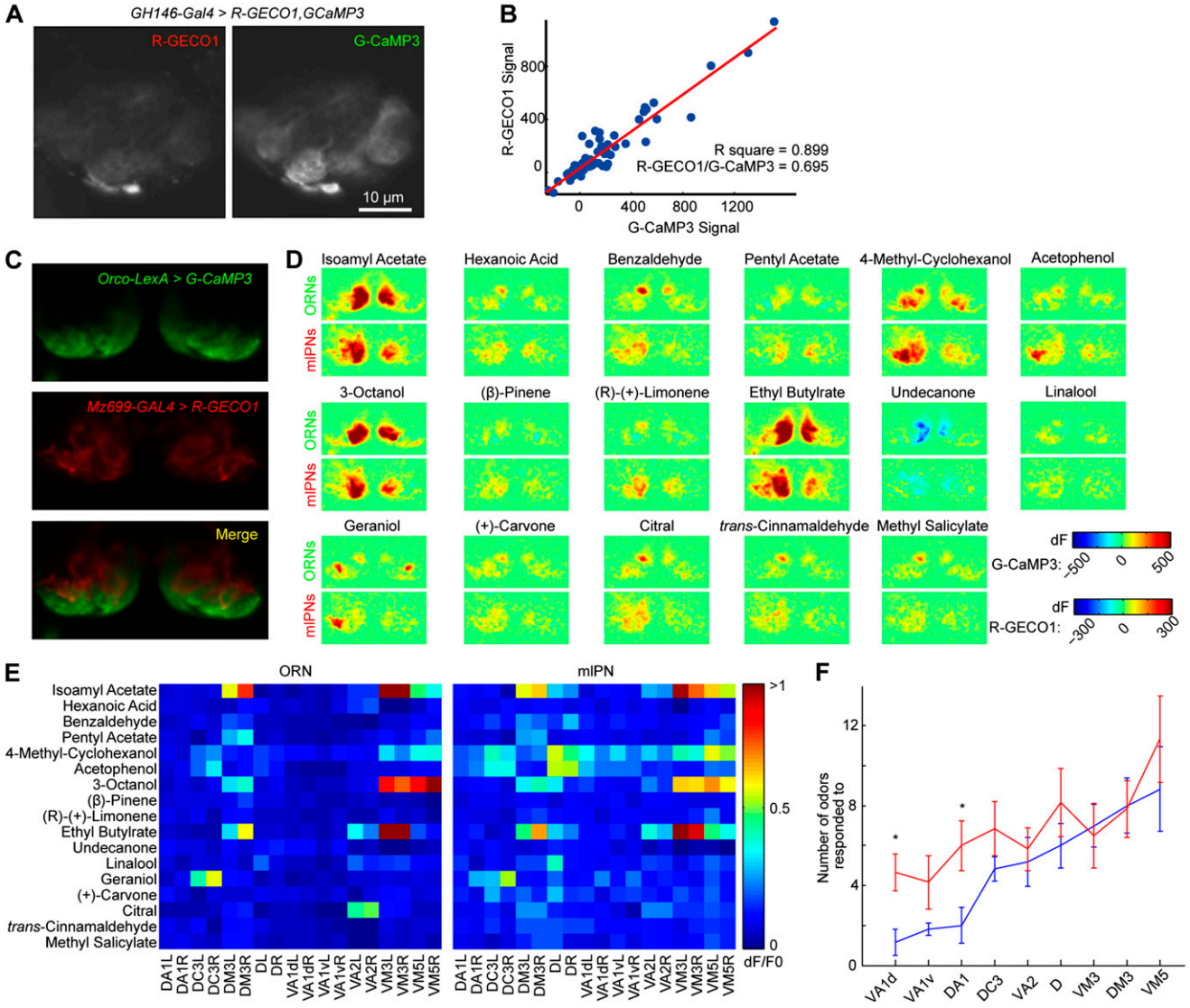

Fig. S3. Correlated odor-evoked activities in olfactory receptor neurons (ORNs) and Mz699-mlPNs, as well as robust odor-evoked activities in mlPN3s. (*A* and *B*) The calcium indicators R-GECO1 and G-CaMP3 expressed in the same group of mPNs showed similar expression patterns (*A*) and correlated dynamics (*B*) in the presence of different odor stimulations. The response amplitude of R-GECO1 measured as absolute change of fluorescence intensity is about two-thirds that of G-CaMP3. (*C*) Fluorescence images showing optical sections of antennal lobes in which large fractions of mlPNs and ORNs were labeled with R-GECO1 (red) and G-CaMP3 (green), respectively. (*D*) Sample false-color images illustrating the odor-evoked fluorescence changes of mlPNs or ORNs in one brain (the scale is shown by the color bars at *Lower Right*). (*E*) Color maps summarizing the averaged amplitude of odor-evoked responses in ORNs and mlPNs in defined glomeruli. Glomeruli in the two brain hemispheres are illustrated separately, as indicated by "L" (left) and "R" (right) at the end of each glomerular name ($n = 4$ brains). (*F*) Plots showing the averaged number of odors that activated mlPNs (red) or ORNs (blue) in the indicated glomeruli ($n = 8$ ALs; mean ± SEM; $^*P < 0.05$).

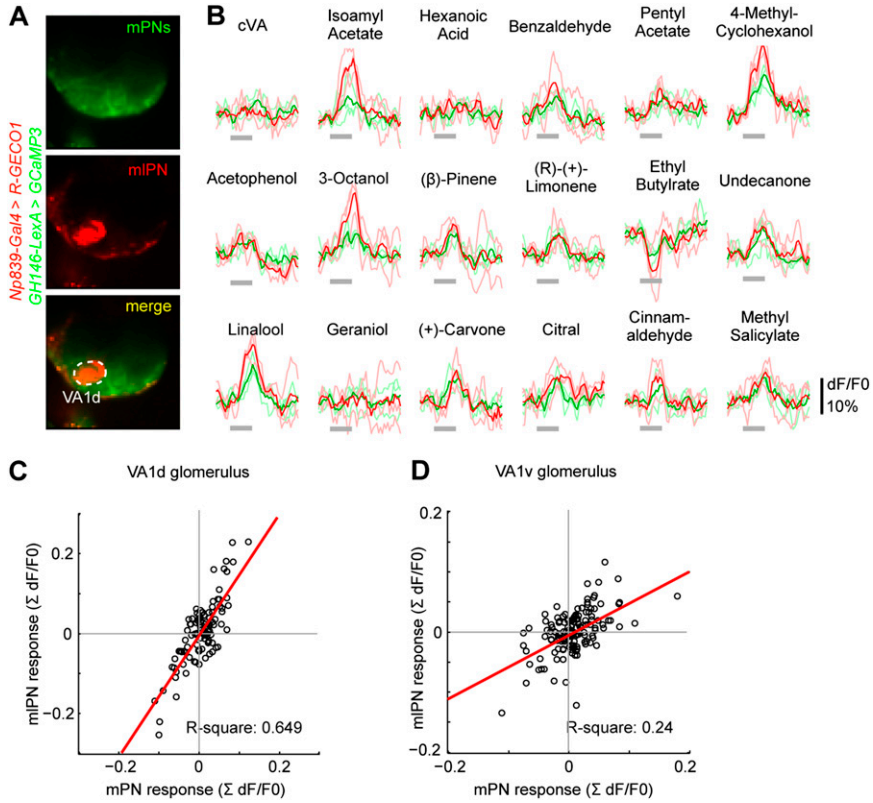

Fig. S4. Comparable odor response profiles exhibited by mlPN1s and mPNs innervating the same single glomerulus as shown by dual-color calcium imaging. (*A*) Fluorescence images of an AL where *Np839-Gal4*–labeled mlPN1s expressed R-GECO1 and *GH146-LexA*–labeled mPNs expressed G-CaMP3. The glomerulus innervated by the two types of labeled PNs (VA1d) is indicated by a dashed circle. (*B*) Traces showing the responses of mlPN1s (red) and mPNs (green) in VA1d to the indicated odors. Darker traces were averaged from three lighter traces. Gray bars below the traces indicate presentation of the odor stimuli (2 s). The two types of PNs exhibited comparable response profiles. (*C*) The response amplitude in mlPNs is plotted against that in mPNs. The odor-evoked activities in the two types of PNs were positively correlated. Red line is a linear fit (108 responses from six pairs of PNs). (*D*) Similar to *C*, except that the responses in mlPN1s and mPNs innervating the VA1v glomerulus are plotted (108 responses from six pairs of PNs).

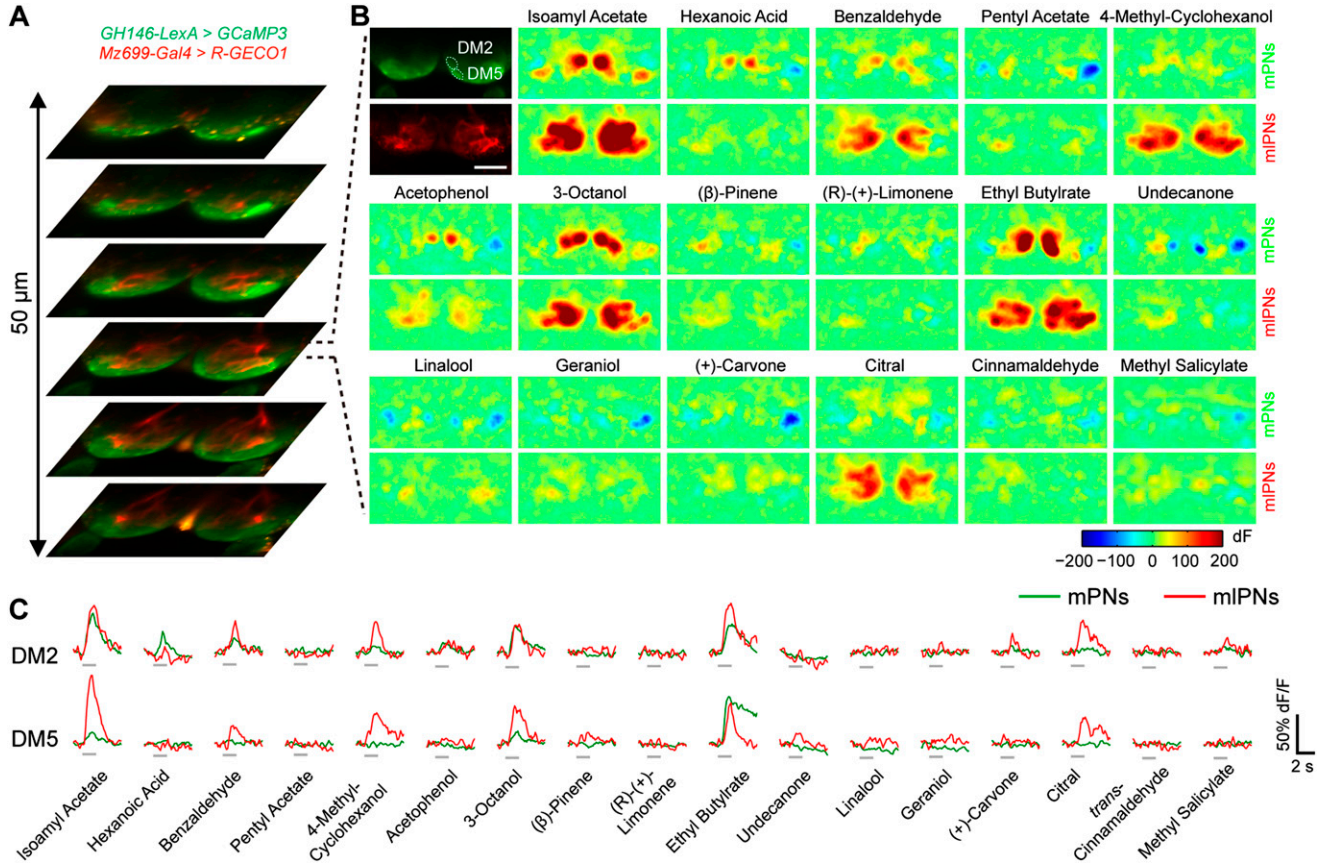

Fig. S5. Odor-evoked activities in mlPN2s and mPNs are overlapping and correlated. (*A*) Sample image stacks of ALs where mlPNs and mPNs were labeled with R-GECO1 (red) and G-CaMP3 (green), respectively. Images were taken at different depths with an interval of 10 μm. (*B*) Confocal images showing the baseline fluorescence (*Top Left*) (Scale bar, 20 μm.) and false-color images showing the odor-evoked fluorescence changes in the dendrites of mlPNs and mPNs. (*C*) Example odor-evoked response traces (dF/F_0) of mlPNs and mPNs innervating the DM2 and DM5 glomeruli, as indicated by dashed circles in *B*, *Top Left*. Gray bars below traces indicate the presentation of odor stimuli (2 s).

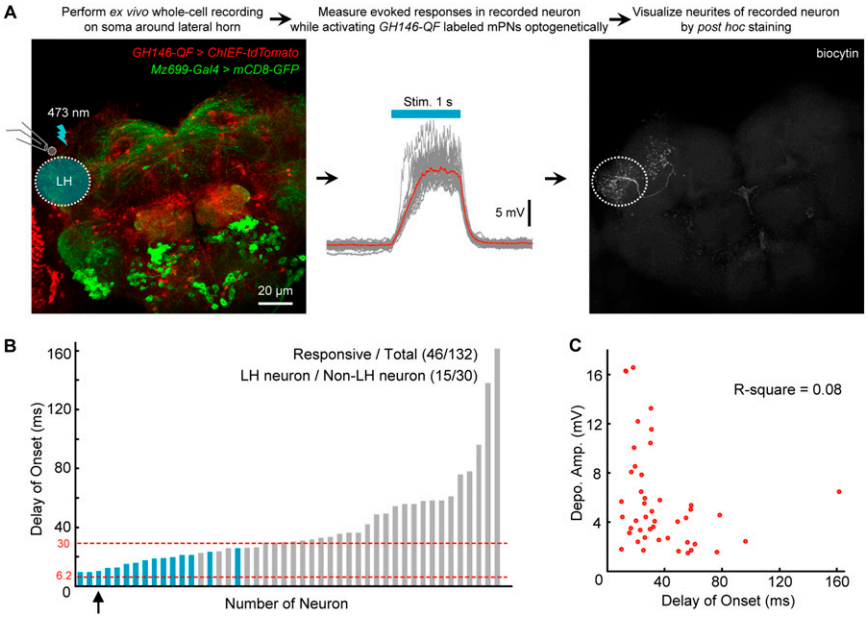

Fig. S6. Identification and characterization of LH neurons downstream of mPNs. (*A*) Experimental procedures performed to identify neurons downstream of mPNs. First, whole-cell recording was performed on neurons surrounding LH in brains of the indicated genotype (*Left*). Then laser stimulation (2.39 mW) was immediately provided to illuminate LH or the ipsilateral AL while responses in the recorded neuron were measured (*Center*). If no obvious response was detected, the electrode was withdrawn with the recorded soma, and new electrodes were used to patch other neurons until an obvious response was detected. After getting successful access to a responsive neuron, biocytin or neurobiotin was loaded into the neuron by providing hyper- or depolarizing current (0.5 s at 1 Hz) for a prolonged period (~2 h). Finally, the morphology of the recorded neuron was visualized after performing post hoc staining (*Right*). Note that the *GH146-QF* line contains a sequence that drives DsRed expression under synthetic P3 promoters, which explains the global DsRed signal found in the brain. (*B*) In total, 132 neurons from 55 brains were recorded, and 46 of these neurons showed detectable laser-evoked responses with variable delays of onset. Examination of the projection patterns of most of the responsive neurons (45/46) showed that about one-third of these neurons (15/46, blue bars) innervated LH, whereas the remaining neurons (30/31, gray bars) did not. The average delays of onset in responsive neurons are plotted. All of the neurons with neurites innervating LH (blue bars) had relatively short delays. Arrow indicate the neuron shown in *A*. Red dashed lines indicate the shortest and longest delays of first spiking in *GH146-QF*–labeled mPNs under laser illumination. (*C*) The response amplitude is plotted against delay of response onset. No clear correlation was found.

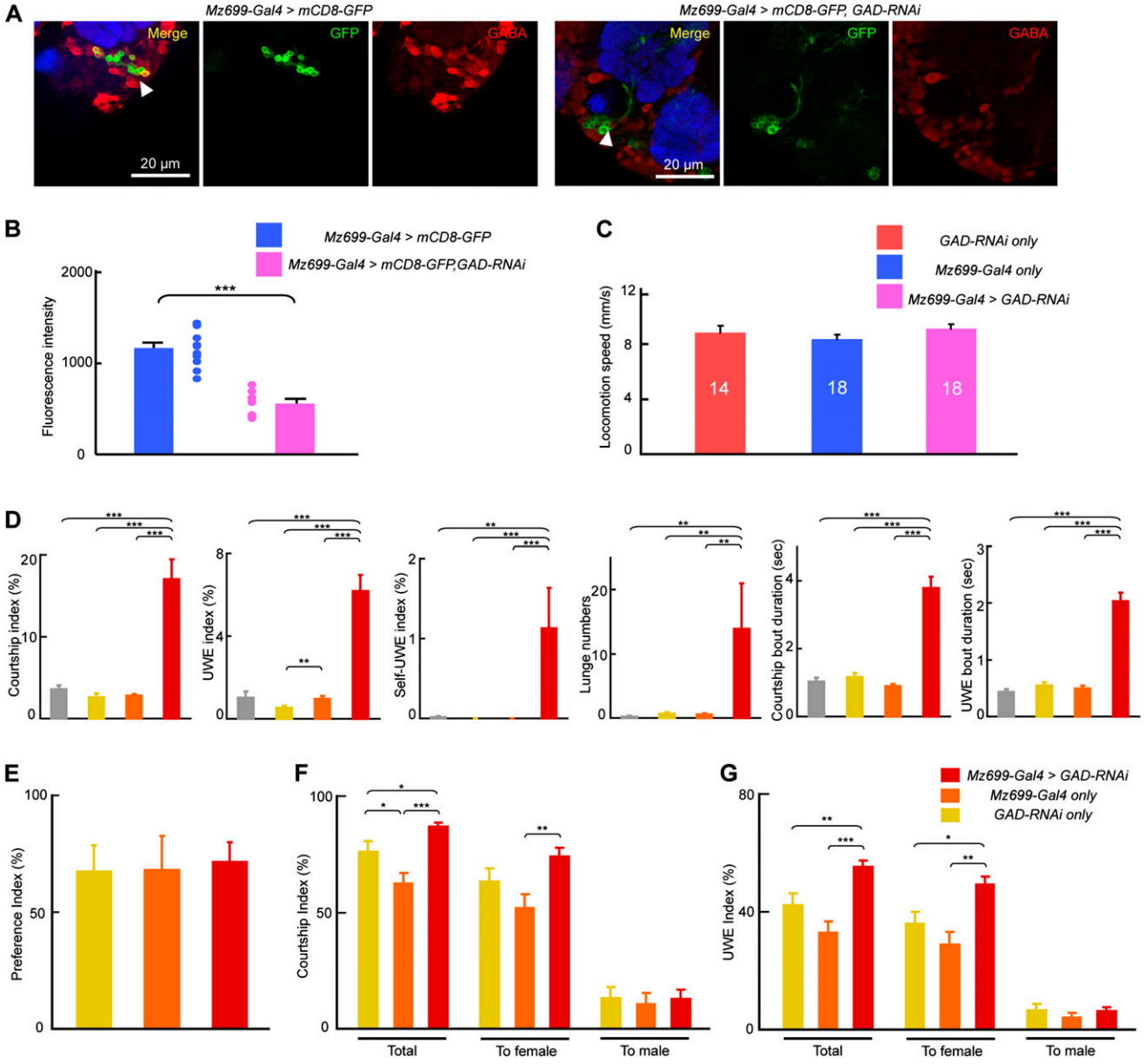

Fig. S7. Efficient down-regulation of GABA in Mz699-mlPNs affected male behavior. (*A*) Sample fluorescence images of brains of the indicated genotypes. In a control brain (*Left*), most GFP-labeled mlPNs were GABA positive (arrowheads). By coexpressing GAD-RNAi in these GFP-labeled mlPNs, the GABA level was greatly reduced (*Right*). (*B*) Summary plot showing that the expression of GAD-RNAi efficiently down-regulated the level of GABA in the somata of mlPNs, indicated as the decrease of fluorescent intensity of GABA signals in mlPN somata in knockdown brains (mean ± SEM, $n = 12$ for control brains and $n = 8$ for knockdown brains; $***P < 0.001$). (*C*) Bar plots illustrating the running speed of flies of different genotypes. Sample numbers are indicated within the bars. No significant difference was found between groups. (*D*) Bar plots summarizing courtship index, unilateral wing extension (UWE) index, self-UWE index (exhibition of UWE without turning toward another fly), number of lunges, duration of courtship bouts, and duration of UWE bouts in male pairs of the indicated genotypes in 10 min. $n = 10$ for wild-type pairs, $n = 20$ for the other three genotypes. Mean ± SEM is shown. $**P < 0.01$; $***P < 0.001$. (*E–G*) Bar plots showing the preference index (*E*), courtship index (*F*), and UWE index (*G*) of individual males of the indicated genotypes toward two decapitated targets with opposite genders. $n = 17$ for *GAD-RNAi* only males, $n = 19$ for *Mz699-Gal4* only males, and $n = 20$ for *Mz699-Gal4* > *GAD-RNAi* males. Total indices in *F* and *G* are the sum of the index toward females and the index toward males, respectively. Mean ± SEM is shown. ($*P < 0.05$; $**P < 0.01$; $***P < 0.001$).